Taylor & Francis
Taylor & Francis Group

Vehicle System Dynamics
International Journal of Vehicle Mechanics and Mobility

ISSN: (Print) (Online) Journal homepage: https://www.tandfonline.com/loi/nvsd20

Implementation of a variable-geometry suspension-based steering control system

Dániel Fényes, Máté Fazekas, Balázs Németh & Péter Gáspár

To cite this article: Dániel Fényes, Máté Fazekas, Balázs Németh & Péter Gáspár (2022) Implementation of a variable-geometry suspension-based steering control system, Vehicle System Dynamics, 60:6, 2018-2035, DOI: 10.1080/00423114.2021.1890798

To link to this article: https://doi.org/10.1080/00423114.2021.1890798

Published online: 23 Feb 2021.

VEHICLE SYSTEM DYNAMICS
2022, VOL. 60, NO. 6, 2018–2035
https://doi.org/10.1080/00423114.2021.1890798

Implementation of a variable-geometry suspension-based steering control system

Dániel Fényes[a], Máté Fazekas[a], Balázs Németh[b] and Péter Gáspár[b]

[a]Department of Control for Transportation and Vehicle Systems, Budapest University of Technology and Economics, Budapest, Hungary; [b]Systems and Control Laboratory, Institute for Computer Science and Control (SZTAKI), Eötvös Loránd Research Network (ELKH), Budapest, Hungary

ABSTRACT

The paper proposes the implementation of a control system for a variable-geometry suspension to achieve steering functionality. The implementation is performed in a Hardware-in-the-Loop (HiL) simulation environment with a unique suspension test bed. The purpose of the control system is to achieve path-following functionality for the vehicle with automatic steering based on the proposed system. The paper proposes the design and the implementation of a hierarchical control system. The high-level control is responsible for the computation of the requested steering angle, and the low-level control aims to realise the steering angle through the intervention of the linear actuator in the suspension system. The effectiveness of the proposed control system is demonstrated through HiL simulation examples.

ARTICLE HISTORY
Received 11 September 2020
Revised 16 December 2020
Accepted 7 February 2021

KEYWORDS
Variable-geometry suspension; Hardware-in-the-Loop simulation; controller implementation; model predictive control

1. Introduction and motivation

In the recent decade, variable-geometry suspension systems have gained attention in the area of automotive research. The term *variable-geometry suspension* refers to a group of suspension systems with different purposes and functionalities, rather than a specific construction. The common principle of the suspension is that the effectiveness of functionality is achieved by the modification in the geometry of the construction. In the following, the most important variable-geometry suspension construction types are summarised.

Increased steering functionality is achieved through the modification of the tilting angle of the wheel, as it is realised in the prototype Mercedes F400 [1]. In the construction, the suspension is equipped with an actuator, which can tilt the wheel directly, i.e. the camber angle of the wheel is modified, which generates a lateral force on the tyre. The direct tilting control can be especially useful for sports cars which have low height and are designed for high speed. Through direct tilting, handling safety and driving fun can be improved. Furthermore, the tilting of the wheel can also be modified by changing the lateral position of the suspension arm [2,3]. The modification of the suspension arm position can be carried out by using an electro-hydraulic actuator [4] or an electric motor [5]. The main

CONTACT Balázs Németh balazs.nemeth@sztaki.hu

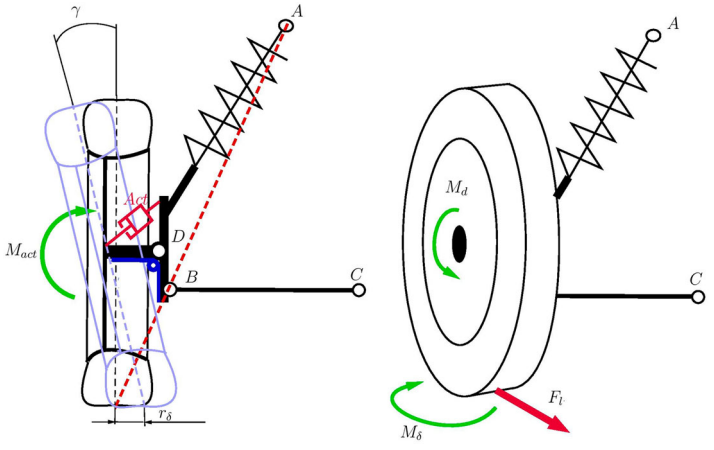

Figure 1. Concept of the variable-geometry suspension.

goal of this construction is to improve both the lateral and vertical dynamics of the vehicle. Another solution can be found in [6,7]. In this construction, the toe angle of the rear axle is modified through an electro-mechanical actuator, which is fixed to the lower suspension arm and modifies the position of the wheel using an additional assist link. This mechanism can improve the driving stability of the vehicle. Intervention in the suspension geometry can also be achieved through the modification of the spring-damper unit position [8,9]. Through the modification of the connection, the stiffness of the suspension can be modified, with which travelling comfort, road holding, pitch and roll dynamics can be improved.

The scheme of another important type of variable-geometry suspension, which is the focus of this paper, is found in Figure 1. The goal of this construction is the improvement of lateral dynamics based on the tilting of the wheel, which generates the rotation of the wheel for steering purposes. Although the tilting does not generate significant lateral tyre force directly, the induced rotation of the wheel has a high impact on lateral dynamics [10–12].

The idea behind this suspension is briefly summarised as follows. Figure 1 shows the basic structure of the suspension is close to the McPherson suspension construction. Joints A and B define the steering axis of the suspension, which is denoted by the dashed line. Scrub radius r_δ of the suspension is depicted by the distance between the steering axle and the contact point of the tyre (where it reaches the ground). The scrub radius is determined by the construction and thus, r_δ can be changed by the modification of the camber angle (γ). For this purpose, an actuator is used, which can modify the camber angle through the rotation of the wheel around joint D. Therefore, the longitudinal force F_l with r_δ generates a moment M_δ, which can rotate the wheel around the steering axis:

$$M_\delta = F_l r_\delta, \tag{1a}$$

$$\ddot{\delta} = \frac{M_\delta}{I_\delta}, \tag{1b}$$

where I_δ denotes the inertia of the steering axis. For example, if r_δ is set to be zero, the steering angle of the wheel is unchangeable. But, if r_δ is modified, the left or right steering

of the wheel depending on the sign of r_δ is achieved. Thus, the aim of the control is to set the camber angle with which the requested steering angle is achieved.

The advantages of the presented suspension are the integration possibility with an in-wheel electric drive and the functionality of independent steering. Through the integration with in-wheel drive torque vectoring intervention can be achieved, and thus, independent steering with independent driving can increase the manoeuvrability of the vehicle. Moreover, it provides the possibility of reconfiguration, which can be important for safety reasons in automated vehicles.

The paper proposes the implementation of the control systems on variable-geometry suspension based on a quarter-car test bed with one wheel in the Hardware-in-the-Loop (HiL) environment. A test bed in SZTAKI (Institute for Computer Science and Control) was built in the last years to verify the effectiveness of the proposed variable-geometry suspension control, which has been examined previously through high-fidelity simulations [2,3,10]. To the best of the authors' knowledge the implementation of the control on this type of variable-geometry suspension in a real test bed is unique. The contribution of the paper is a hierarchical control algorithm whose effectiveness during the implementation has been demonstrated. The hierarchical control structure contains high- and low-level control algorithms. The high-level control is responsible for path tracking, which is implemented in the high-fidelity simulation environment CarMaker. The role of the low-level control is to set the steering angle using a linear actuator in the test bed. The paper demonstrates that the proposed concept of the variable-geometry suspension is able to realise steering functionality.

The paper is organised as follows. The variable-geometry suspension test bed concerning the structures of the construction and the control algorithms is proposed in Section 2. Section 3 proposes the design of the control algorithm, i.e. the design of the high-level control for path following and the design of the low-level control for positioning the wheel. The analysis and the experimental tuning of the low-level control are presented in Section 4. The effectiveness of the control systems through HiL simulation is demonstrated in Section 5. Finally, Section 6 forms the conclusions and the future challenges of the paper.

2. Structure of the variable-geometry suspension test bed

The test bed for variable-geometry suspension is presented in two ways. First, the construction of the test bed with the most important units is introduced. Second, the architecture of the control system together with the electronic platforms is presented.

2.1. Construction of the test bed

The construction of the test bed follows the concept which is illustrated in Figure 1. Nevertheless, the location of the actuator is modified for constructional reasons, i.e. in the original concept the actuator is placed on the hub of the suspension, while in the test bed the actuator is linked to the frame of the test bed (see Figure 2).

The test bed consists of the following main units:

(1) *Linear actuator* is responsible for the modification of the camber angle. The type of the actuator: LATT 4A 1/12, its supply voltage is 12 V and its stroke is 165 mm. The linear

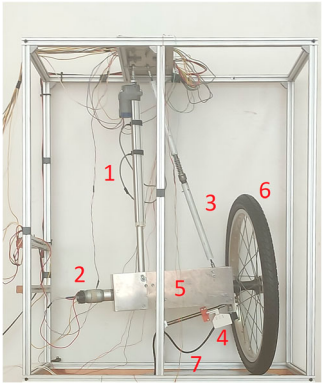

Figure 2. Construction of the test bed.

actuator is also equipped with a hall sensor-based encoder, which is used to determine the current position of the actuator. The actuator has its own electronic board, which controls its position, at a maximum speed of 37 mm/s. In the present construction, the speed of the stroke is constant in both directions. This limitation on actuation is considered in the design of the low-level controller.

(2) *DC motor*, which is used to drive the wheel. The type of the motor is Actobotics 638280, which has a planetary gearbox to ensure adequate torque for the wheel. The supply voltage of this part is 6–12 V, the maximum speed is 313 RPM (Rotation Per Minute) and the maximum load is 3 Nm. Furthermore, the gear ratio is 121/3249. The motor is equipped with an encoder on the motor shaft whose resolution is 48 Countable Events Per Revolution.

(3) The *upper suspension arm* is an essential part of the MacPherson strut. The spring on it ensures the appropriate vertical load for generating the required longitudinal force. The upper arm is linked to the frame through a three-dimensional joint, and it also has a connection to the hub of the suspension.

(4) The *lower suspension arm* is also a crucial part of the MacPherson suspension system. It is linked to the frame through a one-dimensional joint. The other side of the arm is linked to the hub using a three-dimensional joint. On the lower arm, another encoder is found, which is used to determine the steering angle. It actually measures the rotation of the axis of the joint. This encoder works with 5 V current, and its resolution is 3–480 LPI (Lines Per Inch). It represents the resolution of 0.18°.

(5) The *hub* contains the bearing of the shaft, whose sketch is illustrated in Figure 3. The left side of the shaft is linked to the motor (2) through a clutch, which can compensate for the eccentricity in the connection of the shafts. On the other side, the shaft is coupled to the wheel. Moreover, the hub has connections to the linear actuator and both to the upper and lower arms (see Figure 3).

(6) The *wheel* of the test bed has a diameter of 18”, which is generally used for bicycles. The wheel is rigidly linked to the shaft of the hub, which means that it rotates at the same speed as the motor. The wheel can be rotated in both forward and reverse directions.

(7) The *rotating plate* is the lower part of the suspension test bed, which can rotate around the vertical axis. Its purpose is to guarantee the rotating motion and the limited displacement of the wheel, which are generated by the driving and steering effects.

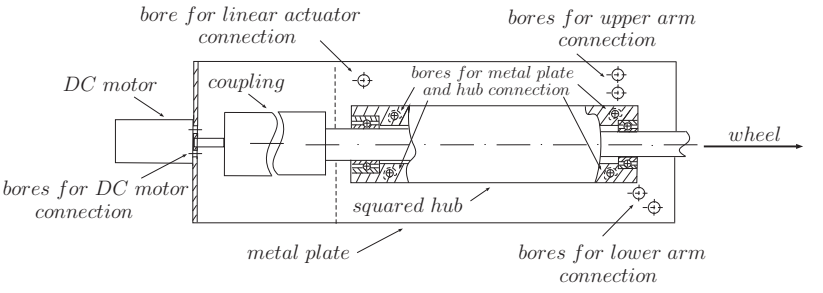

Figure 3. Sketch of a hub for the illustration of bearing.

The goal of the test bed is to verify the effectiveness of the variable-geometry suspension control, which is proposed in this paper. Due to the limited control-oriented requirements, the test bed has the following limitations.

- The steering angle of the wheel is limited. This limitation is resulted from the limited wheel speed and the limited achievable camber angle, which is generated by the linear actuator. The achievable steering angle is between $\pm 20^{\circ}$.
- The limitation of the wheel speed is resulted from the constructional reasons of the in-door test bed. The achievable maximum longitudinal speed for vehicle dynamic simulations is 27 km/h, which is resulted from the 313 RPM maximum rotation speed of the DC motor.
- The actuation speed of the linear actuator is 37 mm/s, which bounds the realisable vehicle manoeuvres. Moreover, the set of realisable manoeuvres is determined by the time delay in the operation of the test bed (see Section 4). It is also considered that the actuator is able to carry out the requested motion since the lateral load on the wheel of the test bed is small.
- The wheel has low elasticity, which means that the pneumatic trail of the wheel in the formulation process of the test bed model is neglected.
- A further limitation of the test bed is resulted from the rolling plate, which is flat. Thus, the effectiveness of the control against the roughness of the road cannot be evaluated.

In spite of these assumptions, the proposed test bed can be used for the analysis of the variable-geometry suspension control strategy under limited vehicle dynamic scenarios with reduced longitudinal velocity.

2.2. Hardware-in-the-Loop control architecture

In order to test the presented test bed a Hardware-In-the-Loop setup has been developed. The dynamics of the whole vehicle is modelled by the high-fidelity simulation software, CarMaker. The design of the setup involves additional components, as shown in Figure 4. The main components of the setup are the following.

- The *computer* has two features in the HIL simulation. First, it contains the CarMaker and the Matlab/Simulink simulation environments. The main purpose of the CarMaker

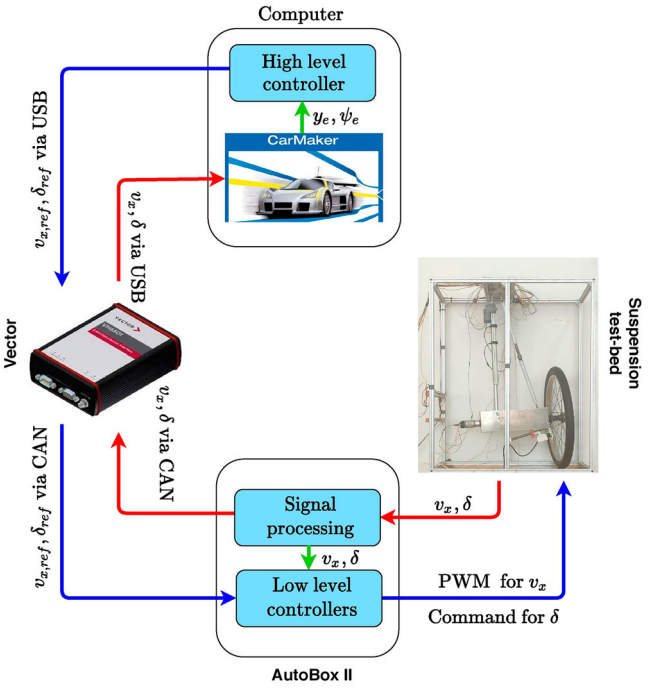

Figure 4. Hardware in the loop setup.

software is to model lateral, vertical and longitudinal dynamics of the vehicle excluding the steering dynamics, which is realised in the test bed. CarMaker receives the processed measured signals: longitudinal velocity (v_x) and the steering angle δ. Using these measurements, the software computes the errors (y_e, ψ_e) of the lateral position and the yaw angle from the current position of the vehicle and the predefined road. Second, the computer contains high-level control, which is also implemented in the Matlab/Simulink environment. It computes the reference signals for longitudinal velocity $v_{x,ref}$ and the steering angle δ_{ref}. All the signals (received and computed) are transmitted through a serial communication protocol from/to the vector device.

- The *vector interface* is responsible for transmitting the measurements from the sensors towards the computer, on which the CarMaker and the Simulink are run. Vice versa, the computed reference signals are also transmitted through this device to the next device, which is the AutoBox.
- The *AutoBox II* is an essential part of the setup. It serves several purposes: It is responsible for processing the raw signals from the sensors placed on the suspension system (the position of the actuator, the velocity of the wheel, and the realised road wheel angle). The lower level controller is also implemented on this device. The lower level controller computes the PWM signal for the DC motor and the command for the linear actuator. The AutoBox also transmits the measured and processed signals to the vector device through CAN communication. This device also receives the reference signals from the vector device.

3. Hierarchical control design for variable-geometry suspension

The proposed control system is ordered into a hierarchical structure, as is also shown in Figure 4. The low-level controller is responsible for the realisation of the desired steering angle (δ_{ref}), and moreover, for the required longitudinal velocity ($v_{x,ref}$). This controller is implemented on the AutoBox device. Meanwhile, the high-level controller computes the reference steering angle δ_{ref} using the processed measurements and the computed errors (y_e, ψ_e) from the CarMaker software.

The paper mainly focuses on proving the effectiveness and operation of the proposed variable geometry suspension ; therefore, only the lateral control design is presented here. The reference longitudinal velocity is set at a constant value during the tests. The tracking of that given constant velocity is carried out by a PID controller, which is implemented on the AutoBox device. The design of the longitudinal controller is not detailed in the paper; the applied method can be found in [13,14].

3.1. Design of lateral controller on the high level

Since the purpose of the control design is to guarantee the trajectory tracking of the vehicle, the one-track bicycle model is used as the basis of the lateral controller. This model consists of three dynamical equations, which describe the lateral, the yaw and the longitudinal motions of the vehicle [15].

$$mv_x(\dot{\psi} + \dot{\beta}) = C_1\alpha_1 + C_2\alpha_2, \tag{2a}$$

$$J\ddot{\psi} = C_1\alpha_1 l_1 - C_2\alpha_2 l_2, \tag{2b}$$

$$\dot{v}_y = v_x(\dot{\psi} + \dot{\beta}), \tag{2c}$$

where m is the mass of the car, J denotes the yaw-inertia, l_i are geometric parameters, C_i are the cornering stiffness of the front and rear wheels. α_i are the side-slip angles of the front and rear wheels, which can be computed as: $\alpha_1 = \delta - \beta - \frac{l_1\dot{\psi}}{v_x}$ and $\alpha_2 = -\beta + \frac{l_2\dot{\psi}}{v_x}$. Moreover, $\dot{\psi}$ is the yaw-rate, β denotes the side-slip angle of the vehicle and v_i are the longitudinal and lateral velocities of the vehicle.

Using these equations, the following state-space can be built up:

$$\dot{x}_v = A_v x_v + B_v u_v, \tag{3}$$

where u_v consists of the steering angle, the state-vector is $x_v = [\,\beta\ \dot{\psi}\ \psi\ v_y\ y\,]$ and A_v, B_v are system matrices. ψ and y are computed by integrating their derivatives: $\dot{\psi}$ and v_y.

The goal of the high-level control is to guarantee the path tracking of a vehicle on a road segment through automated steering. In the field of steering control design, there are several approaches which can be applied. For example, in [10], a Linear Parameter-Varying (LPV)-based method for variable-geometry suspension-based steering control design is proposed. In the selection of the control method, it is necessary to consider the constraint regarding the path following and the specifications of the test bed.

- In the design of the high-level control, the edges of the road as the constraints on the path must be incorporated.

- The generation of the steering angle has time requirements, i.e. the low-level control and the motion of the suspension result in a delay in the system.

For these reasons, a Model Predictive Control (MPC) algorithm is developed for the control design [16,17]. In the MPC design problem, the constraints can be incorporated. Furthermore, the impact of the delay on the low level can be reduced through the preliminary knowledge on the reference path.

The MPC method requires a discrete-time state-space representation of the model. Therefore, the presented state-space model is converted to a discrete one using the sample time T_s. Then, the discrete-time state-space representation can be formulated as

$$x_v(k+1) = \phi_v x_v(k) + \Gamma_v u_v(k), \tag{4}$$

where ϕ_v and Γ_v are the matrices of the discretised system.

The prediction of the motion of the vehicle must be performed for the horizon n, which can be computed as (see [18])

$$\begin{aligned} z_{pred}(k,n) &= \begin{bmatrix} z(k+1) \\ z(k+2) \\ \vdots \\ z(k+n) \end{bmatrix} \\ &= \begin{bmatrix} 0 & 0 \\ 0 & 0 \\ 1 & 0 \\ 0 & 0 \\ 0 & 1 \end{bmatrix}^T \begin{bmatrix} \phi_v \\ \phi_v^2 \\ \vdots \\ \phi_v^n \end{bmatrix} x_v(k) \\ &\quad + \begin{bmatrix} 0 & 0 \\ 0 & 0 \\ 1 & 0 \\ 0 & 0 \\ 0 & 1 \end{bmatrix}^T \begin{bmatrix} \Gamma_v & 0 & \cdots & 0 \\ \phi_v\Gamma_v & \Gamma_v & \cdots & 0 \\ \vdots & \ddots & \ddots & \vdots \\ \phi_v^{n-1}\Gamma_v & \phi_v\Gamma_v & \cdots & \Gamma_v \end{bmatrix} \begin{bmatrix} u_v(k) \\ u_v(k+1) \\ \vdots \\ u_v(k+n-1) \end{bmatrix}. \end{aligned} \tag{5}$$

The goal of the control design is to guarantee the trajectory tracking of the vehicle, which consists of two main components: the tracking error of the lateral position y_e and the tracking error of the yaw-angle of the road ψ_e (see Figure 5). The errors of tracking can be expressed as

$$e(k,n) = z_{ref}(k,n) - z_{pred}(k,n), \tag{6}$$

where $e(k,n)$ is a vector, which contains both error signals.

Using this error vector, the following cost function can be determined, which must be minimised in order to guarantee the trajectory tracking of the vehicle:

$$J = \frac{1}{2} e(k,n)^T Q e(k,n) + U(k,n)^T R U(k,n), \tag{7}$$

where $U(k,n) = [\, u_v(k) \ \ldots \ u_v(k+n-1) \,]^T$. Moreover, Q and R are weighting matrices, which guarantee a balance between tracking performance and control actuation (steering angle).

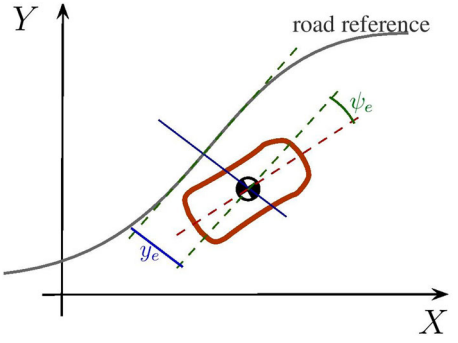

Figure 5. Illustration of the tracking errors.

Using (5) and (6), the cost function can be transformed to

$$J = U(k,n)^T \sigma U(k,n) + \nu^T U(k,n), \tag{8}$$

where σ and ν are matrices.

Finally, the following quadratic optimisation task must be solved to obtain the optimal control input sequence:

$$\min_{U(k,n)} U(k,n)^T \sigma U(k,n) + \nu^T U(k,n) \quad s.t. \begin{cases} B_b < H_{in} U < B_u, \\ l_b \leq u_i \leq l_u. \end{cases} \tag{9}$$

However, the vehicle and the steering system have their own bounds; therefore, the minimisation problem is subject to constraints. B_b and B_u are constraints of the states of the system, such as the edges of the road and the limitations of the yaw-rate signal. In the meantime, l_i guarantees that the computed control input does not exceed the limitations of the steering system. The matrix H_{in} is formed as

$$H_{in} = \begin{bmatrix} \Gamma_v & 0 & \cdots & 0 \\ \phi_v \Gamma_v & \Gamma_v & \cdots & 0 \\ \vdots & \ddots & \ddots & \vdots \\ \phi_v^{n-1} \Gamma_v & \phi_v^{n-2} \Gamma_v & \cdots & \Gamma_v \end{bmatrix}. \tag{10}$$

The vectors B_b and B_u are

$$B_b = \begin{bmatrix} x_{v,low}(t+1) \\ \vdots \\ x_{v,low}(t+n-1) \end{bmatrix} \quad B_u = \begin{bmatrix} x_{v,up}(t+1) \\ \vdots \\ x_{v,up}(t+n-1) \end{bmatrix}, \tag{11}$$

where $x_{v,low}(T)$ denotes the lower limits of the states at the time step T and $x_{v,up}(T)$ denotes the upper limits of the states at T.

The computed vector of the input signals U contains the requested control inputs on the horizon ahead of the vehicle. In the implementation of the controller, the first element u_v of U is applied. It represents the steering angle, which must be actuated so that the vehicle follows the path. Nevertheless, u_v cannot be achieved directly, so that the steering

angle must be generated through the modification of the scrub radius. Therefore, in the hierarchical structure of the control system, u_v is a reference signal for the low-level control, such as

$$\delta_{ref} = u_v. \tag{12}$$

3.2. Design of suspension controller on the low level

The purpose of the low-level control design is to guarantee the tracking of the reference steering angle through the intervention of the linear actuator. The performance problem is formulated as

$$z_s = \delta_{ref} - \delta \quad |z_s| \rightarrow \min! \tag{13}$$

The starting point of the low-level control design for guaranteeing the tracking performance is the consideration of the dynamics of suspension system (1). The dynamics on the steering is formed as

$$\ddot{\delta} = \frac{F_l r_\delta}{I_\delta}. \tag{14}$$

The relation between the scrub radius and the camber angle can be handled as a linear function [19], such as

$$r_\delta = k_1 \gamma, \tag{15}$$

where k_1 is a constant parameter. Moreover, in the presented test bed the relation between the camber angle and the position of the linear actuator can also be approximated by a linear function [10]:

$$\gamma = k_2 d, \tag{16}$$

where d is the position of the linear actuator and k_2 is the parameter. Therefore, the dynamics between the position of the actuator and the steering angle can be formulated as

$$\ddot{\delta} = \frac{F_l k_1 k_2 d}{I_\delta}. \tag{17}$$

For control design purposes, the presented dynamics can be transformed into the Laplace domain (s) as

$$G(s) = \frac{\Delta(s)}{D(s)} = \frac{F_l k_1 k_2}{I_\delta s^2} = \frac{K}{s^2}, \tag{18}$$

where $\Delta(s)$ is the Laplace transformation of $\delta(t)$ and $D(s)$ is the Laplace transformation of the position of the linear actuator $d(t)$.

As it can be seen, the dynamics of the suspension system can be handled as a double integrative term. Therefore, the reasonable choice can be a derivative controller, which can ensure the tracking of the reference signal and also makes the operation of the controller fast. The controller $C(s)$ is formulated as

$$C(s) = Ps, \tag{19}$$

where P is the tuning parameter. The input of the controller $C(S)$ is the error of the steering angle e_δ and its output is the position signal for the linear actuator. The structure of the controller is illustrated in Figure 6.

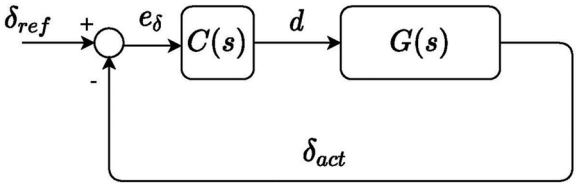

Figure 6. Outer loop in the low-level control.

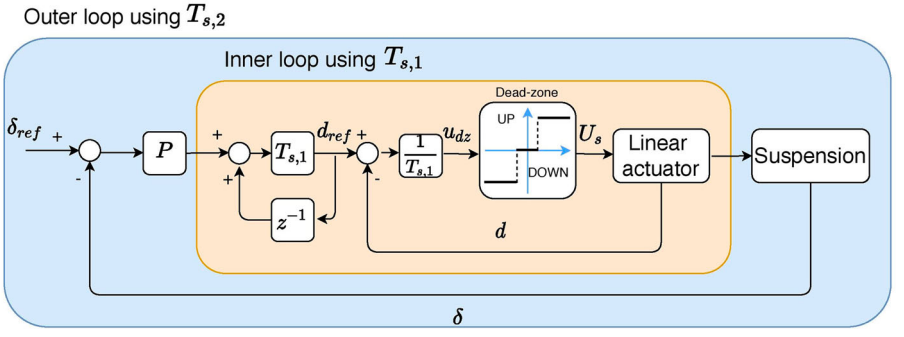

Figure 7. Architecture of the low-level controller.

Since the implementation of the low-level control in the Hardware-In-the-Loop simulation is realised in discrete time, the presented controller (19) is implemented using the sampling time $T_{s,2}$. But, in the implementation, it must be considered that the control board of the linear actuator has only two control intervention possibilities (see Section 2.1). Therefore, the presented control structure must be extended in order to achieve an improved tracking performance. It leads to a cascade control structure, in which the outer loop contains (19) and the inner loop is responsible for handling the actuator limitations and avoiding the chattering effect. The structure of the low-level controller can be seen in Figure 7.

As it can be seen, the inner loop has two main parts. In the first part, a virtual reference signal is computed, which must be tracked by the linear actuator. This reference signal is computed as the integral of the input of the inner loop using the sampling time $T_{s,1}$ as

$$d_{ref}(k) = P\sum_{j=1}^{k}(e_\delta(j))T_{s,1} = P\sum_{j=1}^{k}(\delta_{ref}(j) - \delta(j))T_{s,1}, \tag{20}$$

where T_{s_1} denotes the sampling time of the inner loop controller and P is the tuning parameter (see (19)). Then, the input for the dead-zone is determined as

$$u_{dz} = (d_{ref} - d)/T_{s,1}. \tag{21}$$

Remark 3.1: The motivation behind the formulation of (20) can be illustrated as follows. If $P = 1$ is selected and $T_{s,1}$ is infinitesimally small, the expression of the sum in (20) is transformed into an integral expression: $\int_0^t e_\delta(\tau)\mathrm{d}\tau$. Since the tracking of the position is considered to be fast, the integral is expressed as $\int_0^t e_\delta(\tau)\mathrm{d}\tau = d(t)$, which leads to $e_\delta(t) =$

$\dot{d}(t)$, which relationship has similarity to (17). Therefore, this algorithm can be considered as a derivative controller with respect to e_δ. Note that in order to guarantee the fast-tracking of the position, the sampling time of the inner loop controller must be smaller than the sampling time of the outer loop controller ($T_{s,1} \ll T_{s,2}$).

The computed signal u_{dz} cannot be applied directly to the linear actuator. The electronic board of the actuator has three designated pins for controlling the actuator: up, down and stop. These three control signals are ordered into a vector $U_s = [up, down, stop]$. The signal u_{dz} is transformed to impulse signals through a dead-zone, which is formed as

$$\begin{cases} \text{if } u_{dz}(n) > dz_{high} \text{ then } U_s = [1,0,0], \\ \text{if } u_{dz}(n) < dz_{low} \text{ then } U_s = [0,1,0], \\ \text{otherwise,} \qquad\qquad U_s = [0,0,1], \end{cases} \tag{22}$$

where dz_{high} and dz_{low} are the limits of the dead-zone and 1 denotes an impulse signal on the specific pin of the electric board.

Remark 3.2: Dynamical equation (1) shows that longitudinal force on the wheel also has an impact on the steering angle. Thus, the setting of δ can be formed as a control problem with two interventions, i.e. a coupled control of the longitudinal force and wheel tilting. An example of the coupled control design method is found in [10]. Since the accurate control of the longitudinal force can result in difficulties due to the constructional limitation of the given quarter-car test bed, in the proposed applied control method, pure wheel tilting as an individual intervention is realised.

4. Experimental tuning of the low-level controller

Since the dynamics of the test bed contains several nonlinearities and uncertainties, which makes the tuning of the controller hard, the value of the parameter P is determined experimentally through test cases. Before the tuning process, an example is presented to show the efficiency of the proposed inner loop controller.

In the test scenario, a sinusoidal signal is chosen as a reference signal and the parameter P is chosen $P = 1$, which is related to $\dot{d}_{ref} = e_\delta$. The test scenario is performed on $v_x = 25$ km/h, which is equal to 300 RPI of the wheel. Figure 8 shows the tracking of the reference signal.It can be seen that the inner loop control algorithm is able to guarantee the required fast-tracking performance. Small oscillation can be observed in the figure, which is caused by the applied numerical derivative method.

In the following, the tuning of the parameter P is presented. In the test cases, the parameter P is modified between $P \in \{30 - 100\}$. During the tests, the control system must ensure the tracking of a predefined reference steering angle. The results are shown in Figures 9 and 10. As the Figures illustrate, at low P value, the tracking is smoother than at high P. However, at low P, the system has a significant delay. The averaged tracking errors and the averaged delays are summarised in Table 1.

As it can be seen, the smallest averaged error belongs to the $P = 30$ case, while the highest one is at $P = 100$. The shortest delay is observed in the case $P = 100$ and the longest one is from the case $P = 30$. Therefore, a balance must be found between delay and accuracy.

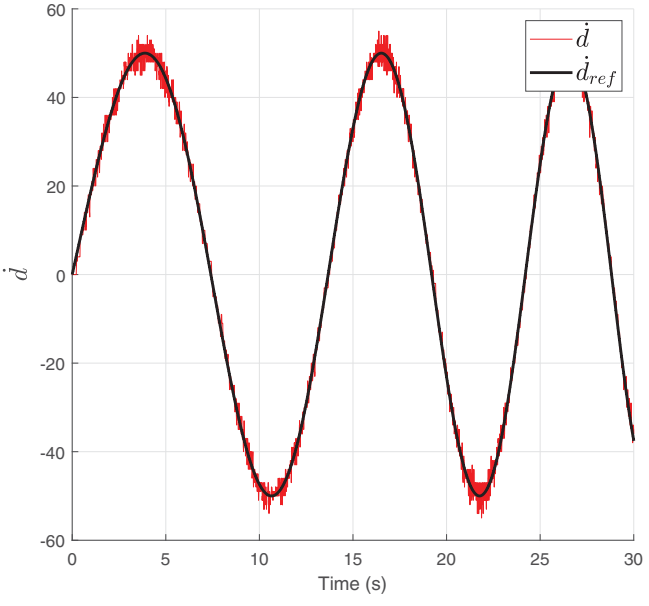

Figure 8. Test of the inner loop controller.

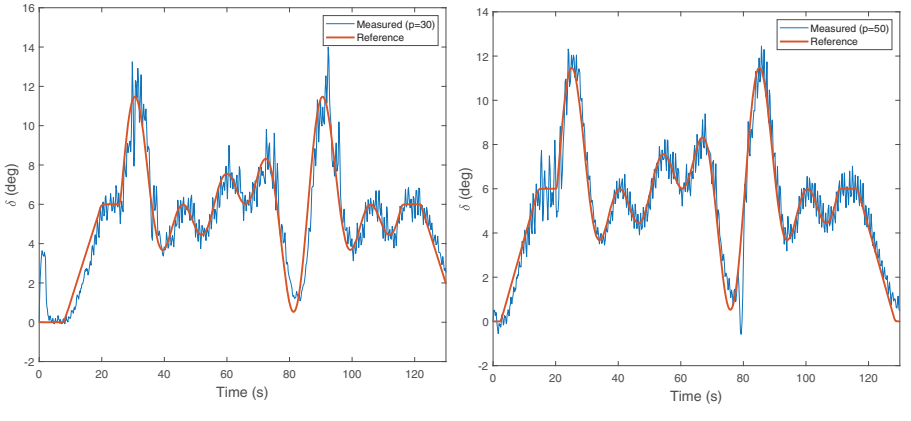

Figure 9. Tests using (a) $P = 30$ and (b) $P = 50$.

Table 1. Tests using different P.

P	Avr. error (deg.)	Avr. delay (s)
30	1.0072	1.11
50	1.0209	0.75
70	1.2028	0.68
100	2.0442	0.61

Note that even the shortest delay is significant ($t_d = 0.61$ s), which is caused by the applied linear actuator. As described in Section 2, the maximum speed of the cylinder is limited ; thus, the delay of the tracking cannot be reduced below a certain value. However, this delay can be compensated for by the presented MPC-based high-level controller,

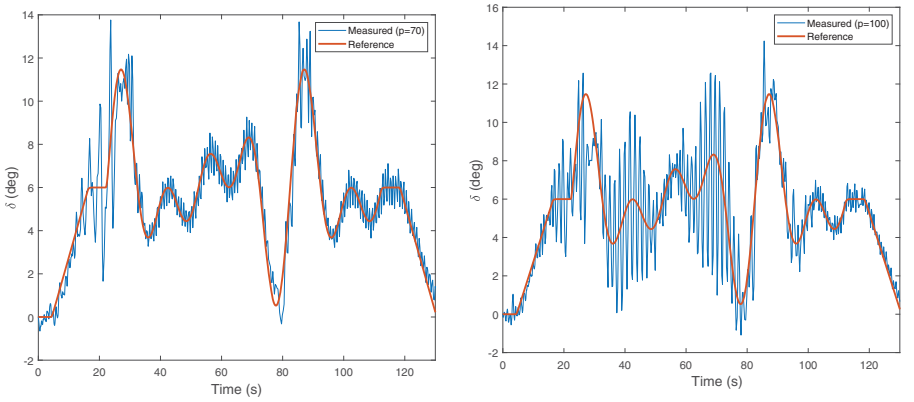

Figure 10. Tests using (a) $P = 70$ and (b) $P = 100$.

i.e. the reference signal z_{ref} for the road tracking is shifted forwards. It results in the enlargement of the feasible set of manoeuvres.

5. Simulation example in Hardware-in-the-Loop test

In this section, a comprehensive Hardware-in-the-Loop simulation example is presented to show the effectiveness and operation of the presented variable geometry suspension system. In the CarMaker software, a D-class car is chosen, whose mass is 1534 kg. The front wheels of simulated vehicles are directly controlled by the measured steering from the test bed. The speed of the front wheels is also directly controlled using the measured speed value. The parameter P is set at 50, since at this value, the linear actuator has no significant oscillation and its time-delay is still low. The sample time of the controller system is set at $T_s = 1$ kHz. The video recording about the operation of the control system on the test bed is found in https://youtu.be/S7cerDwAicI.

During the test scenario, the vehicle must follow a predefined road, which includes sharp bends, as shown in Figure 11(a). As the figure illustrates, the vehicle is able to track the

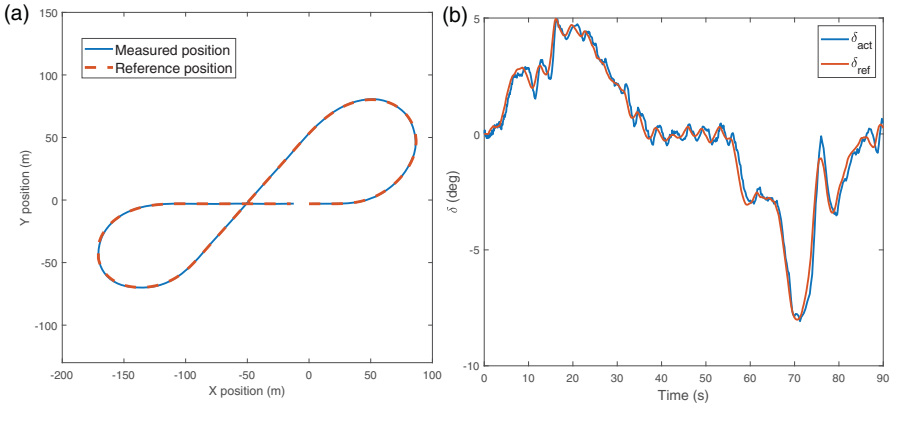

Figure 11. Path and steering angle of the vehicle. (a) Path of the vehicle and (b) steering angle.

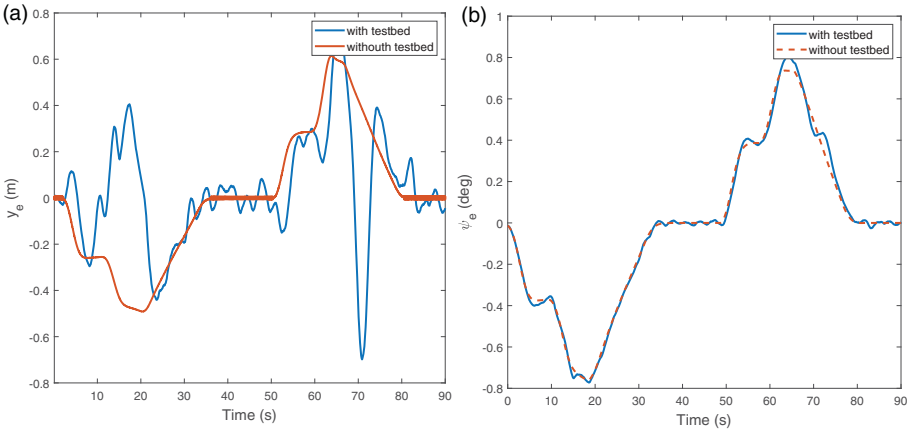

Figure 12. Tracking errors. (a) Error of lateral position and (b) error of yaw-angle.

predefined road at both bends. Figure 11(b) shows the reference and the realised steering angles. The tracking of the steering angle is accurate; however, some oscillations appear at the straight segments. This oscillation is caused by the linear actuator since it works close to its limitations.

Figure 12 depicts the errors of the lateral tracking error and the yaw-angle tracking error. For comparison purposes, the results of the two configurations are presented. The signals *with test bed* present the results of a simulation, whose simulation is performed on the proposed HiL environment. The signals *without test bed* present the results of a simulation, which are related to a configuration without test bed. This configuration contains only the high-level control and CarMaker, and thus, $\delta_{ref} = \delta$. The role of this comparison is to examine the influence of the test bed in the entire simulation scenario. As it can be seen from Figure 12(b), the yaw-angle errors in both signals are close to each other and they have small values, i.e. $\psi_e < 1^\circ$. Nevertheless, in the case of the lateral position, the errors are increased in both cases. Due to the limited capacity of the linear actuator of the test bed, the lateral error has increased variation, but the tendency of the signals are the same. Thus,

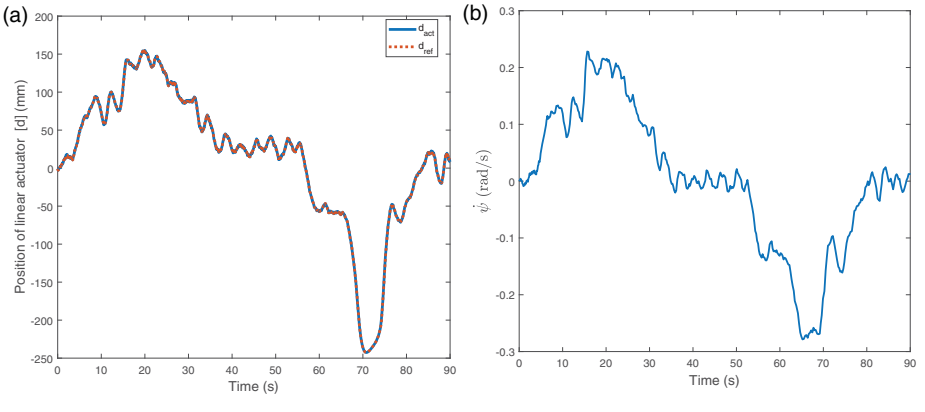

Figure 13. Position of (a) the linear actuator and (b) yaw-rate signal.

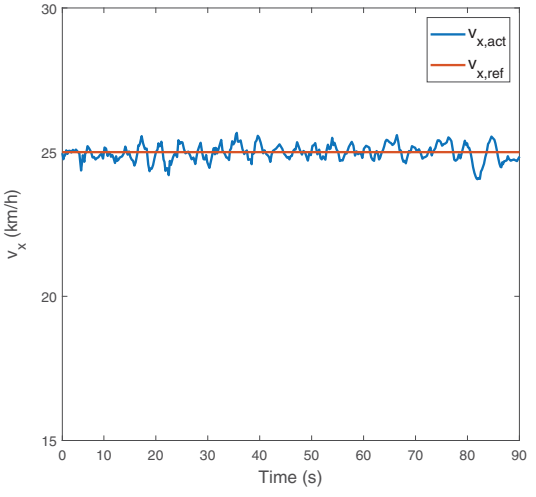

Figure 14. Longitudinal velocity.

the real dynamics of the test bed differs from the dynamics of the conventional simulated steering system in CarMaker, but the low-level control is able to provide an appropriate tracking functionality.

Figure 13 demonstrates the position of the linear actuator and the yaw-rate angle. As it can be seen, the tracking of the position has a very low error. The yaw-rate signal is noisy due to the measured steering angle, which also contains noises. Nevertheless, this signal remains below < 0.3 rad/s, which is an acceptable value for a passenger car.

Finally, Figure 14 shows the longitudinal velocity of the vehicle. As it can be seen, the reference velocity is set at 25 km/h, which is suited to the capacity of the test bed. There is a small oscillation on the measured signal, which is caused by the structure of the test bed. However, the tracking performance of the longitudinal controller is still acceptable.

6. Conclusion

In this paper, the construction of a variable geometry suspension test bed has been presented. The operation and the effectiveness of the control system through a unique Hardware-in-the-Loop simulation with a test bed have been demonstrated. In the paper, a hierarchical control scheme with two layers has been proposed. The high-level controller has been designed to control the lateral dynamics of the vehicle, which was implemented in MATLAB/CarMaker environment. The low-level algorithm is responsible for tracking the reference steering angle. The simulation has shown that the proposed structure and control architecture have been able to guarantee the trajectory tracking of the vehicle under the test bed conditions of the variable-geometry suspension.

Disclosure statement

No potential conflict of interest was reported by the author(s).

Funding

The research reported in this paper and carried out at BME has been supported by the National Research Development and Innovation Fund [TKP2020 IES, Grant No. BME-IE-MIFM] based on the charter of bolster issued by the National Research Development and Innovation Office under the auspices of the Ministry for Innovation and Technology. The research was supported by the Ministry of Innovation and Technology NRDI Office within the framework of the Autonomous Systems National Laboratory Program. The work of D. Fényes was supported by the ÚNKP-20-3 New National Excellence Program of the Ministry for Innovation and Technology from the source of the National Research, Development and Innovation Fund. The work of B. Németh was partially supported by the János Bolyai Research Scholarship of the Hungarian Academy of Sciences and the ÚNKP-20-5 New National Excellence Program of the Ministry for Innovation and Technology from the source of the National Research, Development and Innovation Fund.

References

[1] Schiehlen W, Schirle T. Modeling and simulation of hydraulic components for passenger cars. Veh Syst Dyn: Int J Vehicle Mech Mob. 2006;44(Suppl 1):581–589.
[2] Németh B, Gáspár P. Control design of variable-geometry suspension considering the construction system. IEEE Trans Veh Tech. 2013;62(8):4104–4109.
[3] Németh B, Gáspár P. Nonlinear analysis and control of a variable-geometry suspension system. Control Eng Pract. 2017;61:279–291.
[4] Iman M, Esfahani M, Mosayebi M. Optimization of double wishbone suspension system with variable camber angle by hydraulic mechanism. Eng Tech. 2010;4(1):299–306.
[5] Evers W, van der Knaap A, Besselink I, et al. Analysis of a variable geometry active suspension. International Symposium on Advanced Vehicle Control; Kobe, Japan; 2008. p. 350–355.
[6] U Lee. Active geometry control suspension. ATZ Worldwide. 2010;112:4–9.
[7] Lee S, Sung H, Kim J, et al. Enhancement of vehicle stability by active geometry control suspension system. Int J Auto Tech. 2006;7(3):303–307.
[8] Arana C, Evangelou SA, Dini D. Series active variable geometry suspension for road vehicles. IEEE ASME Trans Mechatronics. 2015;20(1):361–372.
[9] Yu M, Arana C, Evangelou SA, et al. Quarter-car experimental study for series active variable geometry suspension. IEEE Trans Control Syst Technol. 2019;27(2):743–759.
[10] Nemeth B, Fenyes D, Gaspar P, et al. Coordination of independent steering and torque vectoring in a variable-geometry suspension system. IEEE Trans Control Syst Technol. 2018;27(5):2209–2220.
[11] Wang J, Wang Q, Jin L, et al. Independent wheel torque control of 4WD electric vehicle for differential drive assisted steering. Mechatronics. 2011;21:63–76.
[12] Hu C, Jing H, Wang R, et al. Fault-tolerant control of FWIA electric ground vehicles with differential drive assisted steering. IFAC-PapersOnLine. 2015;48(21):1180–1185.
[13] Chamraz S, Balogh R. Two approaches to the adaptive cruise control (ACC) design. In: Proceedings of the 29th International Conference 2018 Cybernetics and Informatics. Lazy pod Makytou; 2018. p. 1–6. doi:10.1109/CYBERI.2018.8337542.
[14] Sahputro SD, Fadilah F, Wicaksono NA, et al. Design and implementation of adaptive PID controller for speed control of DC motor. In: 2017 15th International Conference on Quality in Research (QiR): International Symposium on Electrical and Computer Engineering; Nusa Dua; 2017. p. 179–183. doi:10.1109/QIR.2017.8168478.
[15] Rajamani R, Vehicle dynamics and control. Boston, MA: Springer; 2005.
[16] Zhou H, Guvenc L, Liu Z. Design and evaluation of path following controller based on MPC for autonomous vehicle. In: Proceedings of the 36th Chinese Control Conference; Dalian; 2017. p. 9934–9939. doi:10.23919/ChiCC.2017.8028942.
[17] Jalali M, Khosravani S, Khajepour A, et al. Model predictive control of vehicle stability using coordinated active steering and differential brakes. Mechatronics. 2017;48:30–41.

[18] Choi M, Choi SB. Model predictive control for vehicle yaw stability with practical concerns. IEEE Trans Veh Technol. 2014;63(8):3539–3548.
[19] Fenyes D, Nemeth B, Gaspar P. Optimal control design of a variable-geometry suspension with electro-hydraulic actuator. In: Proceedings of IEEE 15th International Symposium on Applied Machine Intelligence and Informatics; Herl'any; 2017. p. 000337–000342. doi:10.1109/SAMI.2017.7880330.